DOI: 10.1021/ma902577m

Macromolecules
ARTICLE

Modeling of Bottle-Brush Polymer Adsorption onto Mica and Silica Surfaces: Effect of Side-Chain Length

Per Linse*,[†] and Per M. Claesson[‡]

[†]*Physical Chemistry, Center for Chemistry and Chemical Engineering, Lund University, Box 124, SE-221 00 Lund, Sweden and* [‡]*Department of Chemistry, Surface and Corrosion Science, Royal Institute of Technology, SE-100 44 Stockholm, Sweden and Institute for Surface Chemistry, P.O. Box 5607, SE-114 86 Stockholm, Sweden*

Received November 23, 2009; Revised Manuscript Received January 11, 2010

ABSTRACT: Adsorption of a series of charged bottle-brush polymers with side chains of different length on solid surfaces is modeled using a lattice mean-field theory. The bottle-brush polymers are modeled as being composed of two types of main-chain segments: charged segments and uncharged segments with an attached side chain. The composition variable X denotes the percentage of charged main-chain segments and ranges from $X = 0$ (uncharged bottle-brush polymer) to $X = 100$ (linear polyelectrolyte). Two types of surfaces are considered: mica-like and silica-like. The mica-like surface possesses a constant negative surface charge density and no nonelectrostatic affinity for either main-chain or side-chain segments, whereas the silica-like surface has a constant negative surface potential and a positive affinity for the side chains of the bottle-brush polymers. With the mica-like surface, at low X the surface excess becomes smaller and at $X \geq 25$ it becomes larger with increasing side-chain length. Hence, the value of X at which the surface excess displays a maximum increases with the side-chain length. However, with the silica-like surface the surface excess increases with increasing side-chain length at all $X < 100$, and the maximum of the surface excess appears at $X \approx 10$ independent of the side-chain length.

Introduction

Linear polymers carrying a large number of covalently attached side chains, also referred to as bottle-brush polymers or comb polymers, have received great interest in recent years.[1−4] Bottle-brush polymers with hydrophilic nonionic side chains may display a large adsorption leading to low nonspecific protein adsorption,[5−8] strongly repulsive steric interactions,[9,10] and low friction forces,[11−14] with friction coefficients comparable to those obtained with efficient biochemical lubricants such as mucin.[15] A good understanding of their adsorption properties and how these are affected by the nature of the surface, the polymer architecture, solution composition, and interference by surfactants and other polymers present in solution is required for successful applications of physisorbed bottle-brush polymer layers. Such aspects have recently been investigated experimentally[9,12,16−21] using bottle-brush polymers synthesized from (i) poly(ethylene oxide) methylethyl methacrylate (PEO_{45}MEMA) and (ii) methacryloxyethyl trimethylammonimum chloride (METAC). The former monomer contains a 45 unit long oligo(ethylene oxide) chain and the latter a permanently charged cationic group. In the literature these polymers are referred to as PEO_{45}MEMA:METAC-X, where X stands for the mol % of charged main-chain segments.

The adsorption of PEO_{45}MEMA:METAC-X polymers on mica and silica surfaces differs significantly.[9,19] On mica, the low charge density bottle-brush polyelectrolytes ($X \leq 2$) do not adsorb and the maximum adsorption is achieved for $X = 50$. The adsorption on negatively charged mica surfaces has been suggested to be driven by only electrostatic interactions.[12] On the other hand, maximum adsorption on silica is obtained in the composition range $0 < X < 10$. Furthermore, the adsorption of PEO_{45}MEMA:METAC-X polymers on silica is sensitive to changes in pH and ionic strength, and this has been suggested to be primarily due to variations in the nonelectrostatic affinity between the PEO_{45} side chains and silica.[19−21]

Recently, we have proposed a model based on a lattice mean-field theory applied to branched polymers, which represents the main experimental observations of the adsorption of PEO_{45}-MEMA:METAC-X polymers on mica and silica surfaces.[22] There, (i) the effects of polymer segment sequence, (ii) the influence of nonelectrostatic interactions, and (iii) the role of surface charge density were also addressed. In a related work, Postmus et al.[23] have modeled the adsorption of linear PEO on silica surfaces, also using a lattice mean-field theory. In particular, they have included silica surface charge titration and polymer−surface interaction parameters that depended on the surface deprotonation, which lead to a reduced PEO adsorption with increasing pH and salt concentration in accordance with experiments. Such a more detailed description is necessary to nonparametrically treat the pH-dependent PEO−silica interaction.

The most detailed study of the effect of side-chain length on adsorption properties for bottle-brush polymers is likely that of Pasche et al.[8] They considered polylysine with grafted poly(ethylene oxide) side chains containing about 23, 45, and 114 segments adsorbing on Nb_2O_5 surfaces. They found that for relatively high side-chain densities, the ratio between lysine segments and PEO side chains being in the range 3−10, the adsorbed mass increased with the side-chain length. In contrast, no clear dependence on the side-chain length was found at higher or lower side-chain densities. In this contribution, we theoretically examine the effect of the side-chain length on the adsorbed polymer layer. We use the same model as in our previous study,[22] and our results provide predictions of the adsorption behavior of PEO-MEMA:METAC-X bottle-brush polymers with variable

*To whom correspondence should be addressed.

 Published on Web 01/28/2010

side-chain length on mica and silica surfaces that can be tested by experiments.

Theoretical Model

The adsorption of bottle-brush polymers on planar and negatively charged surfaces was modeled as in our previous study.[22] A self-consistent-field theory initially developed by Scheutjens and Fleer[24,25] and later extended to polyelectrolytes [see e.g. ref 26 and references given therein] and branched polymers[27] was used.

Briefly, the space adjacent to a planar surface is divided into layers, and each layer is further divided into lattice cells of equal size. Within each layer the Bragg−Williams approximation of random mixing is applied, and thus all sites in a layer are equivalent. One lattice cell contains either (i) solvent, (ii) a polymer segment, (iii) a solvated cation, or (iv) a solvated anion. The polymer is composed of a main chain consisting of 200 segments, of which (i) the percentage X is positively charged and (ii) the remaining percentage $100 - X$ is uncharged *and* having a side chain with $r_{\text{side-chain}}$ segments. Figure 1a shows the structure of PEO_{45}MEMA and METAC used to synthesis the PEO_{45}-MEMA:METAC-X bottle-brush polymer. In our coarse-graining, we represented (EO)MEMA with one uncharged segment, METAC with one charge segment, and $(EO)_2$ with one uncharged segment; hence, each chemical unit being of similar volume. Figure 1b illustrates the modeled bottle-brush polymer. In this work, the focus is on how the properties of the adsorbed layer depend on the side-chain length, $r_{\text{side-chain}}$. The surface is considered as having either a fixed surface charge density σ (modeling mica surface) or a fixed surface potential ψ_s (modeling silica surface).

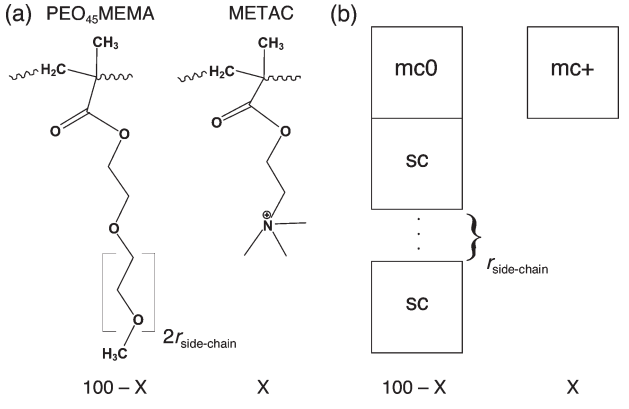

Figure 1. (a) Molecular structures of (left) PEO-MEMA and (right) METAC units of the bottle-brush polymer PEO-MEMA:METAC-X and (b) the coarse-grained model of the two units: (left) the first one composed a uncharged main-chain segment (mc0) and $r_{\text{side-chain}}$ uncharged side-chain segments (sc) and (right) the second one of a positively charged main-chain segment (mc+). X denotes the percentage of METAC units and consequently also the percentage of charged main-chain segments in the copolymer.

There are two different types of interactions in the model: electrostatic (charge−charge) and nonelectrostatic (the rest). The nonelectrostatic interaction between species in adjacent lattice sites is described by Flory−Huggins χ-parameters.[28] The same description is used for the interaction with the surface. Since only the differences of the interaction parameters involving a surface are relevant, we introduce $\Delta\chi_\alpha = \chi_{\alpha,\text{surface}} - \chi_{\text{solvent,surface}}$, α being a main-chain or a side-chain segment. The relation to the adsorption parameter χ_s is given, e.g., for the polymer by $\chi_s = -\lambda_{1,0}\Delta\chi_{\text{polymer}}$, $\lambda_{1,0}$ being the fraction of all neighbors of a site in layer 1, which resides in the surface layer.

In line with the random mixing approximation, charged species (charged polymer segments and salt species) are assumed to interact with an electrostatic potential of mean force, ψ_i, which depends only on the distance to the surface (layer number i). The potential of mean force is related to the charge density through Poisson's equation, $-\varepsilon_0\varepsilon_r\nabla^2\psi_i = \rho_i$, where $\varepsilon_0\varepsilon_r$ is the dielectric permittivity of the medium and ρ_i is the total charge density in layer i. The charges of the species are located to planes in the middle of each lattice layer, and the space in between the charged planes is free of charge. A uniform dielectric permittivity is used.

From the set of volume fraction profiles of the species, $\{\phi_{Ai}\}$, and the interaction parameters, a nonelectrostatic potential u_{Ai} can be calculated for species A in layer i. There is also a layer-dependent but species-independent hard-core potential, u'_i, acting on each species. This potential is essentially the lateral pressure and is responsible for making the volume fraction in each layer sum up to one. Given the nonelectrostatic potential u_{Ai} and the electrostatic energy $q_A\psi_i$ of species A in layer i as well as the hard-core potential u'_i of layer i, the distribution of *unconnected* segments of type A is given by the Boltzmann weight of the sum of the three terms, $\phi_{Ai} \sim \exp[-(u_{Ai} + u'_i + q_A\psi_i)/kT]$. For polymers, the matter becomes more complex since the connectivity has to be taken into account. Finally, since $\{\phi_{Ai}\}$ depends on $\{u_{Ai}\}$ and $\{\psi_i\}$, and $\{u_{Ai}\}$ and $\{\psi_i\}$ are functions of $\{\phi_{Ai}\}$ as indicated above, $\{\phi_{Ai}\}$, $\{u_{Ai}\}$, and $\{\psi_i\}$ have to be solved self-consistently. A numerical solution of this set of implicit and nonlinear equations was carried out using up to 100 layers.

Parameters used in the model calculations of the adsorption of the bottle-brush polymers onto mica-like and silica-like surfaces are compiled in Table 1. Some of the parameters (T, ε_r, X, r_{polymer}, ϕ_{polymer}, and ϕ_{salt}) are known characteristics of experimental systems. The values of some other parameters (d, σ, and ψ_s) are less obvious. Here, we have adopted the lattice cell length $d = 0.5$ nm, the surface charge density $\sigma = -0.2$ for the mica-like surface, and the surface potential $\psi_s = -0.1$ V for the silica-like surface at pH = 6. As to the interaction parameters

Table 1. Model Parameters

quantity	value
temperature	$T = 298$ K
relative dielectric permittivity	$\varepsilon_r = 80$
lattice spacing	$d = 0.5$ nm
degree of polymerization (main chain)	$r_{\text{main-chain}} = 200$
degree of polymerization (side chain)	$r_{\text{side-chain}} = 7, 12, 22, 32$
bulk polymer volume fraction	$\phi_{\text{polymer}} = 1 \times 10^{-4}$
bulk salt volume fraction	$\phi_+ = \phi_- = 3 \times 10^{-4}$
surface charge density[a]	$\sigma = -0.2$ (mica-like surface)
surface potential	$\psi_s = -0.1$ V (silica-like surface)
interaction parameters[b]	$RT\chi_{\text{side-chain,water}} = 1.3$ kJ/mol
	$RT\Delta\chi_{\text{side-chain}} = 0$ kJ/mol (mica-like surface)
	$RT\Delta\chi_{\text{side-chain}} = -10$ kJ/mol (silica-like surface)
conversion factors[c]	$C_{\text{salt}}/\text{M} = 13.3\phi_{\text{salt}}$

[a] Number of elementary charges per d^2. [b] Other interaction parameters are zero. [c] Obtained from the size of a lattice cell.

$\chi_{\text{main-chain,solvent}}$, $\chi_{\text{side-chain,solvent}}$, $\Delta\chi_{\text{main-chain}}$, and $\Delta\chi_{\text{side-chain}}$, (i) we have for simplicity assigned $\chi_{\text{main-chain,solvent}} = \Delta\chi_{\text{main-chain}} = 0$, since for low X the number of side-chain segments grossly exceeds the number of main chain segments and hence the interaction involving the side-chains is more important, and at high X the electrostatics dominates, (ii) adopted $RT\chi_{\text{side-chain,solvent}} = 1.3$ kJ/mol as being a reasonable value for the EO−water interaction,[29] (iii) used $RT\Delta\chi_{\text{side-chain}} = 0$ for the EO−mica interaction, and (iv) $RT\Delta\chi_{\text{side-chain}} = -10$ kJ/mol for the EO−silica interaction at pH = 6. The last two assignments were essentially fitted in our previous study.[22] Experimentally it is known that uncharged PEO brush polymers do not adsorb on mica,[9] whereas they strongly adsorb on silica at pH = 6.[19] Other interaction parameters were set to zero. This set of parameters characterizing the systems was found to well represent experimental data for adsorption of PEO_{45}MEMA:METAC-X on mica and silica surfaces.[22]

The length of the side chains are varied, and results will be given for $r_{\text{side-chain}} = 7$, 12, 22, and 32, which would correspond to PEO-MEMA:METAC-X with PEO side chains containing 15, 25, 45, and 65 EO groups. Polymers with the composition $X = 0$, 5, 10, 25, 50, 90, 95, and 100 are regarded. The polymer is considered to be flexible, and the ordering of charged and uncharged segments of the main chain is random. For a given X the same random sequence is used, independent of other parameters.

On the basis of the volume fraction profiles $\{\phi_{Ai}\}$, the adsorbed amount of species A expressed as the surface excess of species A is evaluated according to $\Gamma_{\text{exe,A}} = \sum_i(\phi_{Ai} - \phi_{\text{A,bulk}})$, where the summation extends over all lattice layers and $\phi_{\text{A,bulk}}$ denotes the bulk volume fraction of species A. The polymer surface excess is given by $\Gamma_{\text{exe}} = \Gamma_{\text{exe,main-chain}} + \Gamma_{\text{exe,side-chain}}$.

Result

Mica-Like Surface. The mica-like surface is characterized as a highly charged surface of constant surface charge density, oppositely charged to that of the bottle-brush polyelectrolyte, and with no nonelectrostatic affinity for main-chain and side-chain segments.

The surface excess Γ_{exe} as a function of the bottle-brush composition X for different side-chain lengths $r_{\text{side-chain}}$ on the mica-like surface is displayed in Figure 2a. Generally, bottle-brush polymers with very low charge and a large number of side chains (low X) do not adsorb due to lack of attraction for the surface. Furthermore, polymers with a high linear change density and few side chains (high X) display only a small surface excess due to electrostatic repulsion among adsorbed polymers dominating already at small amount of adsorbed polymer. Thus, Γ_{exe} displays a maximum located at $X_{\max}$ at intermediate X. The maximum appears at lower X for shorter side-chain (smaller $r_{\text{side-chain}}$); here $X_{\max} \approx 20$ for $r_{\text{side-chain}} = 7$ shifting to $X_{\max} \approx 50$ for $r_{\text{side-chain}} = 32$. Interestingly, at $0 < X < 25$ the surface excess *decreases* with increasing side-chain length, whereas at $25 < X < 100$ the surface excess *increases* with increasing side-chain length. At $X \approx 25$ the surface excess is insensitive to the side-chain length, and this polymer composition acts a pivot point. Naturally, Γ_{exe} (and other properties) becomes independent of $r_{\text{side-chain}}$ at $X = 100$, since then we have a linear polyelectrolyte without side chains.

Another characteristic of the adsorbed polymer layer is the number of side chains of adsorbed polymers per unit area, $n^{\text{exe}}_{\text{side-chain}}$. Figure 2b shows that also $n^{\text{exe}}_{\text{side-chain}}$ displays a maximum at intermediate X, the maximum for a given $r_{\text{side-chain}}$ being similar to $X_{\max}$ for Γ_{exe}. For most compositions, the number of side chains per unit area reduces with increasing side-chain length. The largest sensitivity appears

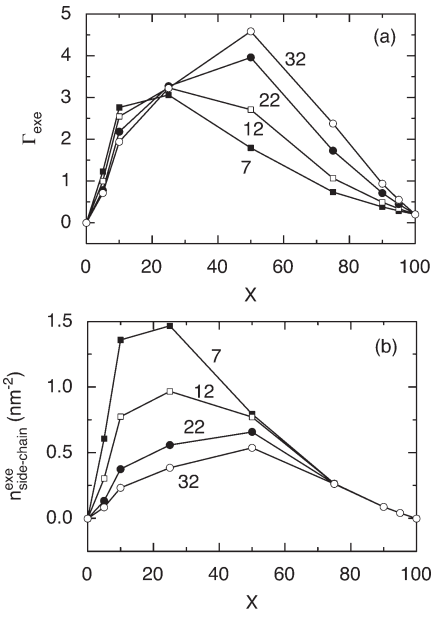

Figure 2. (a) Surface excess Γ_{exe} and (b) excess adsorbed number of side chains $n^{\text{exe}}_{\text{side-chain}}$ as a function of the composition X at the mica-like surface for bottle-brush polymers with side-chain length $r_{\text{side-chain}} = 7$ (solid squares), 12 (open squares), 22 (filled circles), and 32 (open circles). Other parameters as given in Table 1.

at $10 < X < 50$. For $X \geq 50$ with short side-chain length and for $X \geq 75$ with long side-chain length, $n^{\text{exe}}_{\text{side-chain}}$ is independent of $r_{\text{side-chain}}$.

In addition to the surface excess (solid curves), Figure 3a also shows corresponding the surface excess of uncharged systems (dotted curves) and the surface excess corresponding to charge equivalence of the surface charge (dashed curves). As expected, for the uncharged system there is a weak depletion for all X as there is no driving force for adsorption. For sufficiently large X, say $X > X'$, the charges of the excess polyelectrolyte closely balance (but slightly overcompensate) the surface charges, and the adsorption limit for a polymer of a given composition is set by the electrostatics. We notice that X' increases with increasing side-chain length, being $X' \approx 50$ for $r_{\text{side-chain}} = 7$ and $X' \approx 75$ for $r_{\text{side-chain}} = 32$. At $X < X'$ the adsorbed polymers undercompensate the surface charges, and the adsorption limit is governed by the repulsion between the side chains.

The surface potential ψ_s at various X for side-chain lengths $r_{\text{side-chain}} = 7$ and 32 is given in Figure 3b. The magnitude of the surface potential is largest at $X = 0$, since then only small ions screen the surface charges. The magnitude of the surface potential decreases monotonically with increasing X, since polymers with increasing linear charge density and fewer side chains becomes more effective in screening the surface charges. Finally, the transition of large to small $|\psi_s|$ with increasing X appears at larger X for bottle-brush polymers with longer side chains; thus, polymers with the same linear charge density but longer side chains are less effective in screening the surface charge even if their Γ_{exe} is larger (cf. Figures 3a,b). At $X = 0$, $|\psi_s|$ is insensitive to $r_{\text{side-chain}}$, since the bottle-brush polymers are uncharged and depleted from the surface.

There are three factors important for understanding the adsorption data. First, the electrostatic interaction is the sole driving force for the polymer adsorption; in the absence of electrostatic interactions no adsorption occurs (Figure 3a). The strongest electrostatic attraction appears at $X = 100$, at which each main-chain segment possesses a charge. Second,

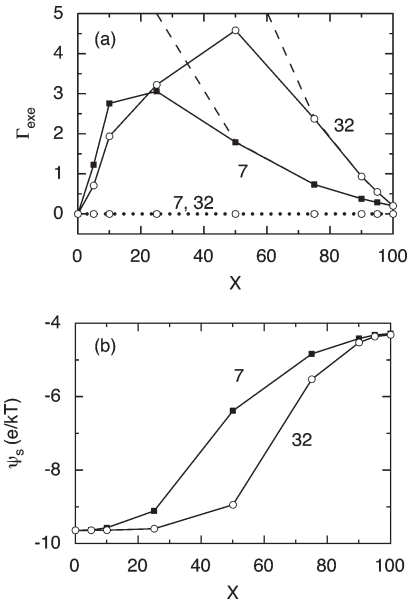

Figure 3. (a) Surface excess Γ_{exe} (solid curves), surface excess without electrostatic interaction (dotted curves), and surface excess corresponding to charge equivalence (dashed curves) and (b) surface potential ψ_s as a function of the composition X at the mica-like surface for bottle-brush polymers with side-chain length $r_{side\text{-}chain} = 7$ (solid squares) and 32 (open circles). Other parameters as given in Table 1.

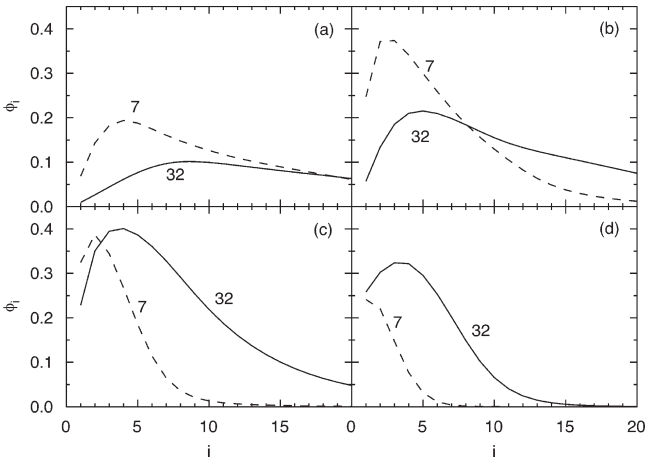

Figure 4. Polymer segment volume fraction ϕ_i as a function of layer number i for (a) $X = 10$, (b) $X = 25$, (c) $X = 50$, and (d) $X = 75$ at the mica-like surface for bottle-brush polymers with side-chain length $r_{side\text{-}chain} = 7$ (dashed curves) and 32 (solid curves). Other parameters as given in Table 1.

the entropic polymer−surface repulsion is another important effective interaction and is largest at $X = 0$, at which each main-chain segment possesses a side chain. Finally, for a given number of adsorbed polymers per unit area, the mass per unit main-chain length and hence the surface excess increase with decreasing X.

(I) Starting at $X = 100$, the increasing Γ_{exe} with decreasing X (Figure 2a) is initially a consequence of increasing mass per unit main-chain length and decreasing polymer charge, owing to basically a preserved charge compensation (Figure 3a). In this *charge compensation regime*, Γ_{exe} is (i) approximately controlled by the polymer−surface charge compensation and (ii) increases with increasing $r_{side\text{-}chain}$. Consistently, the excess adsorbed number of side chains per unit area (Figure 2b) and, thus, the number of adsorbed polymers per unit area are both independent of $r_{side\text{-}chain}$. Furthermore, this regime stretches down to $X = X'$, $X' \approx 50$ for $r_{side\text{-}chain} = 7$, and $X' \approx 75$ for $r_{side\text{-}chain} = 32$ (Figure 3a). The smaller charge compensation regime at the larger $r_{side\text{-}chain}$ appears from the fact that longer side chains exert larger entropic repulsion, remembering that the linear charge density of the bottle-brush polymer is independent of $r_{side\text{-}chain}$.

(II) In the regime $X_{max} < X < X'$, the surface charge starts to become undercompensated (Figure 3a); consequently, $n^{exe}_{side\text{-}chain}$ starts to depend on $r_{side\text{-}chain}$ (Figure 2b), and hence the entropic side-chain repulsion starts to effectively compete with the electrostatic interaction. At this stage, $|\psi_s|$ starts to rise substantially (Figure 3b) due to weaker ability of the polymer to screen the surface charges. The weaker ability of screening the surface charges occurring with the longer side chain at a given X is manifested by both (i) a smaller amount of excess charged main-chain segments and (ii) a location of these segments further away from the surface. The adsorbed amount is still increasing (Figure 2a), since the effect of increasing mass per unit main-chain length still overrides the accelerating charge undercompensation.

(III) Maximum of Γ_{exe} and $n^{exe}_{side\text{-}chain}$ appear at $X = X_{max}$ with X_{max} increasing with $r_{side\text{-}chain}$ (Figure 2a); the $r_{side\text{-}chain}$ dependence is again due to larger entropic repulsion with increasing side-chain length.

(IV) At $X < X_{max}$, Γ_{exe} decreases with decreasing X, since the impact of the increasing entropic repulsion and decreasing electrostatic attraction becomes stronger than the increasing mass per unit main-chain length. The compensation of the surface charges by polymer charges is low, and the surface potential is close to its value at $X = 0$ (Figure 3c).

(V) Interestingly, at $X = 25$ the increasing entropic repulsion and the larger mass per unit main-chain length with increasing $r_{side\text{-}chain}$ balance each other, making Γ_{exe} insensitive to $r_{side\text{-}chain}$.

(VI) At $X < 25$, the electrostatic interaction is so weak that the effect of the entropic repulsion exceeds the effect of the mass per unit main-chain length, making Γ_{exe} to decrease with increasing $r_{side\text{-}chain}$.

Selected polymer volume fraction densities as a function of the layer number, also referred to as polymer volume fraction profiles, for adsorbed polymer layers on mica-like surfaces are given in Figure 4. Generally, the polymer volume fraction maximum appears a few lattice layers away from the charged surface for $X < X''$, whereas for $X > X''$ the volume fraction maximum appear at the surface. The value of X'' increases with increasing side-chain length; here $X'' \approx 75$ for $r_{side\text{-}chain} = 7$ and $X'' \approx 90$ for $r_{side\text{-}chain} = 32$. Noteworthy, at $X = 25$ where the surface excess is insensitive to the side-chain length the polymer volume fraction profiles depend strongly on the side-chain length; viz. for $r_{side\text{-}chain} = 32$ the volume fraction maximum is only haft of the maximum for $r_{side\text{-}chain} = 7$, but the adsorbed polymer layer is thicker for the case with the longer side chain (Figure 4b). At $X = 50$ the two volume fraction maxima are similar, but the adsorbed layer is thicker for $r_{side\text{-}chain} = 32$ (Figure 4c). At $X = 75$ the volume fraction profile for $r_{side\text{-}chain} = 32$ is both denser and thicker as compared to that for $r_{side\text{-}chain} = 7$ (Figure 4d).

Segment density profiles normalized by the corresponding segment density in bulk (far from the surface), referred to as accumulation factors, provide further insight of the structure of the adsorbed polymer layer. Figure 5 shows such accumulation factors of main-chain and side-chain segments for the side-chain length $r_{side\text{-}chain} = 7$ and 32 at $X = 10$, where the abscissa is given in a logarithmic scale to encompass the large variation. Generally the accumulation is large (up to

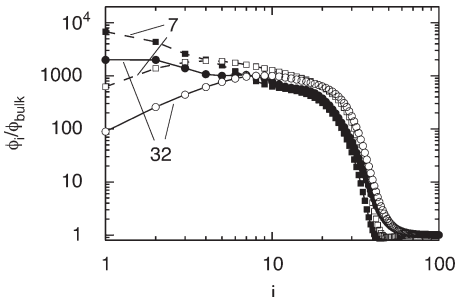

Figure 5. Species volume fraction profiles divided by corresponding bulk volume fraction ϕ_i/ϕ_{bulk} as a function of layer number i for main-chain (solid symbols) and side-chain (open symbols) segments at the mica-like surface for bottle-brush polymers with side-chain length $r_{side\text{-}chain} = 7$ (squares and dashed curves) and 32 (circles and solid curves) at $X = 10$. Other parameters as given in Table 1.

$O(10^4)$) near the surface and decreases to unity in bulk. Near the surface, $i < i'$, accumulation is larger for main-chain segments as a consequence of that some of them being electrostatically attracted by the surface. Further out, $i > i'$, the reverse holds; i.e., here there is a preferred accumulation of side-chain segments. The crossing of the main-chain and side-chain segment accumulation factors appears at $i' \approx 4$ for $r_{side\text{-}chain} = 7$ and at $i' \approx 7$ for $r_{side\text{-}chain} = 32$. Thus, the crossing at i' shifts to larger surface distance as the side-chain length is increased. At the surface the accumulation factor of the main-chain segments exceeds that of the side-chain segments more than 10-fold, this ratio being increased with increasing the side-chain length. The behavior of the accumulation factor at $X = 0$, 50, and 100 for $r_{side\text{-}chain} = 22$ has been discussed earlier.[22] A further analysis shows that at the surface, $i = 1$, the accumulation factors of *charged* main-chain segments are 3−4 times larger than those of the *uncharged* main-chain segments with grafted side-chains.

Thus, the volume fraction profiles a $X = 10$ show that the adsorbed polymer layer is strongly dependent on the side-chain length, even if the surface excesses are similar. As expected, the main-chain segments of the bottle-brush polymer are more strongly accumulated than the side-chain segments at the surface; this is a consequence of some of them being oppositely charged to the surface and the side-chains being uncharged.

Silica-Like Surface. The silica-like surface is also oppositely charged to the bottle-brush polyelectrolyte but possesses a constant surface potential to capture effects originating from the charge regulating ability of the silanol groups. The magnitude of the resulting charge density is always lower than that of the mica-like surface. The side-chain segments, but not the main-chain segments, have a nonelectrostatic affinity to the surface, which is another important difference to the mica-like surface discussed above.

Figure 6a shows the surface excess Γ_{exe} on the silica-like surface as a function of the bottle-brush composition X for different side-chain lengths $r_{side\text{-}chain}$. In comparison to the mica surface, the surface excess is large at small X and its maximum X_{max} occurs between $X \approx 10$ and 20. The surface excess increases with increasing side-chain length; the sensitivity is limited for $X \leq 10$ but becomes substantial in the range $25 < X < 75$. The maximum X_{max} shifts to slightly larger X with increasing $r_{side\text{-}chain}$.

The number of side chains of adsorbed polymers per unit area $n^{exe}_{side\text{-}chain}$ as a function of X is shown in Figure 6b. Also for the silica-like surface, the maximum of $n^{exe}_{side\text{-}chain}$ for a given $r_{side\text{-}chain}$ appears roughly at the same composition as

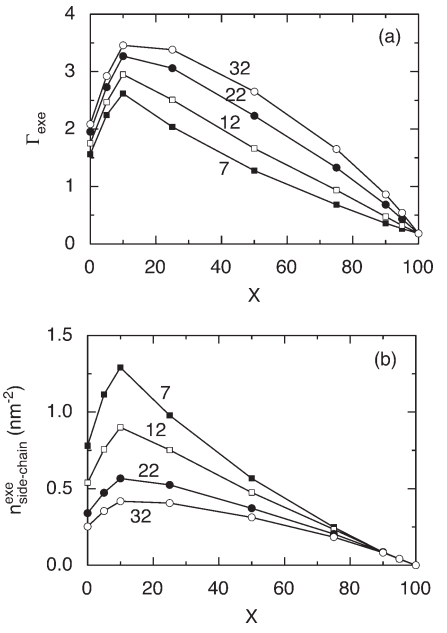

Figure 6. (a) Surface excess Γ_{exe} and (b) excess adsorbed number of side chains $n^{exe}_{side\text{-}chain}$ as a function of the composition X at the silica-like surface for bottle-brush polymers with side-chain length $r_{side\text{-}chain} = 7$ (solid squares), 12 (open squares), 22 (filled circles), and 32 (open circles). Other parameters as given in Table 1.

for the maximum of Γ_{exe}. Furthermore, $n^{exe}_{side\text{-}chain}$ decreases with increasing side-chain length, the largest $r_{side\text{-}chain}$ dependence appearing for $X \leq 50$.

As for the adsorption on the mica-like surface, we will now focus on the adsorption for the side-chain lengths $r_{side\text{-}chain} = 7$ and 32. In contrast to the adsorption on the mica-like surface, Figure 7a displays that Γ_{exe} of uncharged systems (dotted curves) is positive and relatively large. Furthermore, Γ_{exe} is nearly constant at $X \leq 50$ for $r_{side\text{-}chain} = 7$ and at $X \leq 95$ for $r_{side\text{-}chain} = 32$, and the level of the plateau increases with $r_{side\text{-}chain}$. The adsorption for the uncharged systems is obviously driven by the side-chain−surface attraction, and longer side chains preserve the polymers adsorbed with fewer side chains. Returning to the charged system, the surface excess corresponding to charge equivalence of the surface charge (dashed curves) shows that the charges of the excess polyelectrolyte closely balances (but again slightly overcompensates) the surface charges down to X', with $X' \approx 50$ for $r_{side\text{-}chain} = 7$ and $X' \approx 75$ for $r_{side\text{-}chain} = 32$. We note that X' is similar for the adsorption on the silica-like surface as compared to the adsorption on the mica-like surface (cf. Figures 3a and 7a). Although not visible in these graphs, the overcharging is larger on the silica-like surface due to the nonelectrostatic affinity between the side chains and the surface (further discussed in subsection Charge Compensation).

Figure 7b displays the surface charge density σ as a function of X for the two side-chain lengths $r_{side\text{-}chain} = 7$ and 32. The magnitude of the surface charge density increases with increasing X and displays a maximum at $X \approx 90$−95. For most compositions, $|\sigma|$ decreases with increasing $r_{side\text{-}chain}$. The main exception appears when X is near but smaller than 100. At $X = 0$, $|\sigma|$ is insensitive to $r_{side\text{-}chain}$ since the bottle-brush polymers are uncharged. Although they are adsorbed, their different excluded-volume effects on the salt species are negligible.

In addition to the three factors being important for the adsorption on the mica-like surface (given above), two other factors need to be considered to understand the adsorption

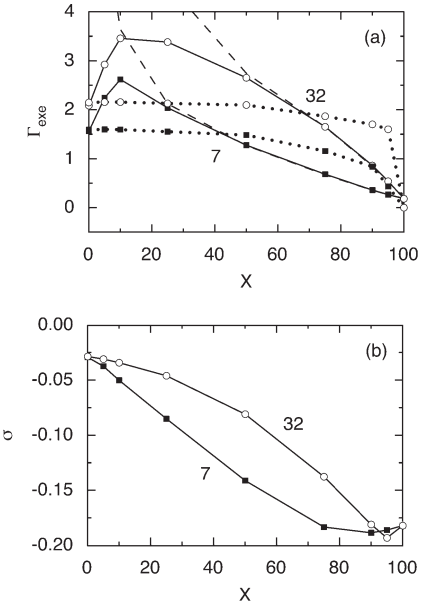

Figure 7. (a) Surface excess Γ_{exe} (solid curves), surface excess without electrostatic interaction (dotted curves), and surface excess corresponding to charge equivalence (dashed curves) and (b) surface charge density σ as a function of the composition X at the silica-like surface for bottle-brush polymers with side-chain length $r_{side\text{-}chain} = 7$ (solid squares) and 32 (open circles). Other parameters as given in Table 1.

on the silica-like surface. The first is the side-chain−surface attraction, which just as the side-chain−surface osmotic repulsion, increases in importance with reducing X. The second is the surface titration, increasing the electrostatic polymer−surface attraction with increasing X.

(I) Again starting at $X = 100$, the charge compensation regime covers compositions down to $X = X'$, $X' \approx 50$ for $r_{side\text{-}chain} = 7$ and $X' \approx 75$ for $r_{side\text{-}chain} = 32$ (Figure 7a). For $X < 100$, the surface excess Γ_{exe} is smaller than for the corresponding uncharged system. Hence, the nonelectrostatic interaction is sufficiently strong to provide a surface excess larger than that corresponding to *charge compensation*; in fact, the electrostatic interaction opposes such a large adsorption. The number of adsorbed side-chains is the same at large X but starts to deviate and decrease with increasing $r_{side\text{-}chain}$ already at $X = 75$ (Figure 6b). This is earlier than for the mica-like surface and is a consequence of the surface titration. Nevertheless, the surface excess increases with increasing $r_{side\text{-}chain}$ (Figure 6a); again, the increasing mass per unit main-chain length well compensates the fewer adsorbed polymers. The magnitude of the surface charge density is large at large X (Figure 7b) due to large accumulation of the oppositely charge bottle-brush polymer. The fact that the largest magnitude appears at $X < 100$ is due to the side-chain−surface attraction. At smaller X, the magnitude of the surface charge density decreases with increasing side-chain length, since the polymers becomes less effective to screen the surface charges. Moreover, the reduced $|\sigma|$ at larger $r_{side\text{-}chain}$ makes $n^{exe}_{side\text{-}chain}$ to become $r_{side\text{-}chain}$ dependent, although Γ_{exe} is still controlled by charge compensation.

(II) In the regime $X_{max} < X < X'$ the surface charge starts to become undercompensated (Figure 7a). The electrostatic interactions and the side-chain−surface attraction cooperatively contribute to the adsorption. This cooperative appearance appears at larger X for larger side-chain length, this being an effect of the larger mass per unit main-chain length with increasing $r_{side\text{-}chain}$.

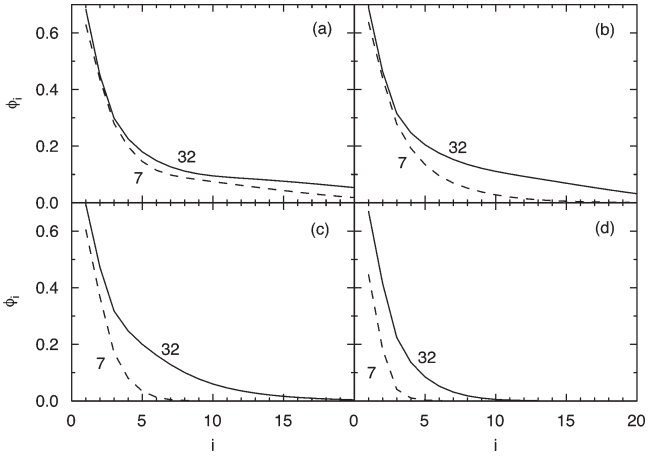

Figure 8. Polymer segment volume fraction ϕ_i as a function of layer number i for (a) $X = 10$, (b) $X = 25$, (c) $X = 50$, and (d) $X = 75$ at the silica-like surface for bottle-brush polymers with side-chain length $r_{side\text{-}chain} = 7$ (dashed curves) and 32 (solid curves). Other parameters as given in Table 1.

(III) Maxima of Γ_{exe} and $n^{exe}_{side\text{-}chain}$ appear at $X = X_{max}$, with X_{max} increasing with $r_{side\text{-}chain}$ (Figure 6). The dependence of X_{max} on $r_{side\text{-}chain}$ is weaker for the silica-like surface than for the mica-like surface. For the mica-like surface, this dependence is a competion between the electrostatic interaction and the entropic repulsion that increases with increasing side-chain length. For the silica-like surface, the side-chain−surface attraction increases in importance with decreasing X and acts in opposition to the entropic repulsion.

(IV) At $0 < X < X_{max}$, Γ_{exe} starts to decrease with decreasing X (Figure 6a), since the effect of the increasing side-chain−surface attraction and increasing mass per unit main-chain length cannot match the combined effect of increasing entropic repulsion and decreasing electrostatic attraction.

(V) The similar Γ_{exe} at $X = 0$ for different side-chain lengths (Figure 6a) shows that the three side-chain length factors discussed under (IV) nearly cancel each other. Furthermore, the magnitude of the surface charge density is small and independent of the side-chain length (Figure 7b), primarily since the bottle-brush polymer is uncharged and the only screening comes from the salt species and second that the excluded-volume effect of the polymer on the salt species is essentially independent of $r_{side\text{-}chain}$.

Figure 8 shows polymer volume fraction densities as a function of the layer number for the same set of X and $r_{side\text{-}chain}$ as for the mica-like surface reported in Figure 4. At $X = 10$ and 25, the polymer volume fraction near the surface is relatively insensitive to $r_{side\text{-}chain}$ and the larger Γ_{exe} at larger $r_{side\text{-}chain}$ stems from a thicker adsorbed polymer layer. At still larger X the polymer volume fraction density at the surface becomes larger with increasing $r_{side\text{-}chain}$. The spatially most extended adsorbed polymer layer is obtained for $X = 10$. As compared to the mica-like surface, the polymer volume fraction is much larger near the surface and the adsorb polymer layer is thinner.

Accumulation factors of main-chain and side-chain segments for side-chain lengths $r_{side\text{-}chain} = 7$ and 32 at $X = 10$ are given in Figure 9. Just as for the mica-like surface, the accumulation factors are large near the surface. At the surface, $i = 1$, accumulation is larger for the side-chain segments; thereafter, a region $1 < i < i'$ is followed where the accumulation is larger for main-chain segments, and eventually a region, $i > i'$, appears where side-chain segmentgs again display the larger accumulation. Thus, we have a three-region division as compared to a two-region division for the

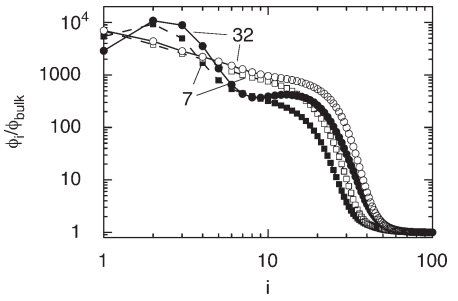

Figure 9. Species volume fraction profiles divided by corresponding bulk volume fraction ϕ_i/ϕ_{bulk} as a function of layer number i for main-chain (solid symbols) and side-chain (open symbols) segments at the silica-like surface for bottle-brush polymers with side-chain length $r_{side\text{-}chain} = 7$ (squares and dashed curves) and 32 (circles and solid curves) at $X = 10$. Other parameters as given in Table 1.

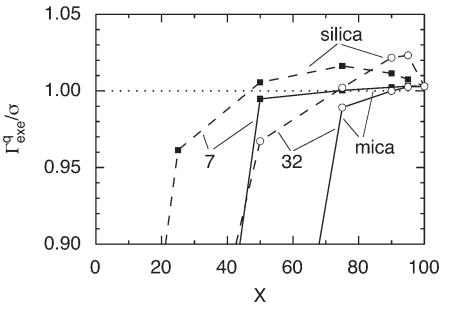

Figure 10. Ratio of surface excess charge and surface charge density (Γ^q_{exe}/σ) as a function of the composition X at the mica-like (solid lines) and silica-like (dashed lines) surface for bottle-brush polymers with side-chain length $r_{side\text{-}chain} = 7$ (solid squares) and 32 (open circles). Other parameters as given in Table 1.

adsorption at the mica-like surface. At the silica-like surface some side-chains are adsorbed, whereas others are stretching away from the surface. The segregation of main-chain and side-chain segments becomes more prominent and i' increases with increasing side-chain length. The appearance of an enriched side-chain volume fraction in layer $i = 1$ is weak for $r_{side\text{-}chain} = 7$, but the accumulation factor of the side-chain segments is 2.3 times that of the main-chain segments for $r_{side\text{-}chain} = 32$.

Hence, the volume fraction profiles of the adsorbed polymer layers at the silica-like surface depends less on the side-chain length as compared to the adsorbed polymer layers on the mica-like surface. An important reason is that the effect of the entropic polymer−surface repulsion is partly compensated by the side-chain−surface attraction that appears in the silica-like system. As a consequence of this attraction, the side-chain segments of the bottle-brush polymer are stronger accumulated than the main-chain segments at the surface.

Charge Compensation. Similarities and differences between the adsorption at the mica-like and silica-like surfaces will further be examined by considering in some more details the ratio of the surface excess charge Γ^q_{exe} and the surface charge density σ. Figure 10 displays this ratio as a function of X for side-chain lengths $r_{side\text{-}chain} = 7$ and 32 for adsorption on the two different surfaces. We previously concluded that at $X > X'$ we had basically a charge compensation; i.e., the charge of the surface excess matches the surface charge density. However, Figure 10 shows that a slight overcompensation of the surface charge occurs in this regime. The overcompensation at $X = 100$, where only electrostatic interactions is present, is very small and in agreement with previous lattice-mean field modeling.[26] As to the mica-like surface this degree of overcompensation remains up to $X = X'$, where a further decrease in X makes the surface charge undercompensated. The drastic transition seen with decreasing X comes from the cooperative effect of the decreasing polymer linear charge density and the increasing number of side chains with increasing X. Furthermore, X' increases with side-chain length because the repulsive steric effect increases with increasing side-chain length. Regarding the silica-like surface, (i) the overcompensation of the surface charge density is larger and (ii) at $X < X'$, but X close to X', the undercharging develops more gradually as compared to that of the mica-like surface. The reason is the additional side-chain−surface attraction, constituting an additional driving force for adsorption that increases in importance with reducing X and the surface charge titration. As mentioned, the nonelectrostatic side-chain−surface attraction and the side-chain−surface entropic repulsion are antagonistic effects. As both effects increase in importance with decreasing X and with increasing $r_{side\text{-}chain}$, the simpler behavior of the surface excess at the silica-like surface mentioned before could be viewed as a consequence of this partial cancellation.

Summary and Outlook

A rich behavior was found for the adsorption of bottle-brush polymers with (i) variable main-chain linear charge density coupled with varying linear side-chain grafting density (described by X) and (ii) variable side-chain length (described by $r_{side\text{-}chain}$) onto mica-like and silica-like surfaces. The mica-like surface had a constant negative surface charge density and no nonelectrostatic affinity for either main-chain or side-chain segments, whereas the silica-like surface had a constant negative surface potential and a positive affinity for the side chains of the bottle-brush polymers. As to the mica-like surface, (i) the electrostatic polymer−surface and polymer−polymer interaction and (ii) the entropic polymer−surface repulsion, dominated by the side-chain−surface repulsion, jointly control the adsorption. In the case of the silica-like surface, the side-chain−surface attraction constitutes a third component affecting the adsorption. Finally, when considering the surface excess Γ_{exe}, concern has to be taken that the polymer mass per unit main-chain length depends on the composition variable X.

We found that the surface excess Γ_{exe} depends on X and $r_{side\text{-}chain}$ in a more complex manner at the mica-like surface as compared to the silica-like surface. At the mica-like surface, the surface excess decreases with increasing $r_{side\text{-}chain}$ at small X and increases at large X. At small X the entropic repulsion among side chains and between side chains and the surface limits the adsorption, and this effect becomes more important for longer side chains. At high values of X it is electrostatics that limits adsorption, and in this regime an increase in side-chain length increases the surface excess due to the increased mass per unit main-chain length. In contrast, at the silica-like surface, where the side-chain interacts favorably with the surface, the surface excess increases with increasing side-chain length *at all X* even though the number of side chains in the adsorbed polymer layer decreases. This is due to the increased mass per unit main-chain length.

In many applications envisaged for bottle-brush polymers with PEO side chains a large PEO content at the solid−liquid interface is considered to be favorable. Our results show that as long as we are in the charge compensation regime long side chains are favorable in this respect. However, when the adsorption is limited by the repulsion between the side chains, the situation becomes more complex. Without a side-chain−surface attraction an increase in side-chain length leads to a reduction in PEO content at the interface when the electrostatic affinity is sufficiently low

($X < 25$ for the mica-like surface). However, when the side-chain−surface affinity is sufficiently attractive, an increase in side-chain length increases the PEO content at the interface (the silica-like case). We further note that the side-chain length significantly affects the structure of the adsorbed polymer layer even when the surface excess is similar. A shorter side chain results in a more compact adsorbed polymer layer. One could expect that such structural differences, and not only the total amount of PEO at the interface, will affect a number of relevant properties such as steric stabilization, lubrication, and nonspecific protein adsorption. Our modeling results provide guidelines for how such effects can be explored in systematic experimental studies.

Acknowledgment. P.L. and P.M.C. acknowledge financial support from the Swedish Research Council (VR).

References and Notes

(1) Zhang, M.; Müller, A. H. E. *J. Polym. Sci., Part A: Polym. Chem.* **2005**, *43*, 3461–3481.
(2) Gorochovceva, N.; Naderi, A.; Dedinaite, A.; Makuska, R. *Eur. Polym. J.* **2005**, *41*, 2653–2662.
(3) Gao, H.; Matyjaszewski, K. *J. Am. Chem. Soc.* **2007**, *129*, 6663–6639.
(4) Krivorotova, T.; Makuska, R.; Naderi, A.; Claesson, P. M.; Dedinaite, A. *Eur. Polym. J.* **2009**, *46*, 171−180.
(5) Huang, N.-P.; Michel, R.; Voros, J.; Textor, M.; Hofer, R.; Rossi, A.; Elbert, D.; Hubbell, J. A.; Spencer, N. D. *Langmuir* **2001**, *17*, 489–498.
(6) Zhou, Y.; Liedberg, B.; Gorochovceva, N.; Makuska, R.; Dedinaite, A.; Claesson, P. M. *J. Colloid Interface Sci.* **2007**, *305*, 62–71.
(7) Perrino, C.; Lee, S.; Choi, S. W.; Maruyama, A.; Spencer, N. D. *Langmuir* **2008**, *24*, 8850–8856.
(8) Pasche, S.; De Paul, S. M.; Vörös, J.; Spence, N. D.; Textor, M. *Langmuir* **2003**, *19*, 9216–9225.
(9) Naderi, A.; Iruthayaraj, J.; Vareikis, A.; Makuska, R.; Claesson, P. M. *Langmuir* **2007**, *23*, 12222–12232.
(10) Dedinaite, A.; Joseph, I.; Gorochovceva, N.; Makuska, R.; Claesson, P. M. *Prog. Colloid Polym. Sci.* **2006**, *132*, 124–130.
(11) Kenausis, L. G.; Voros, J.; Elbert, D.; Huang, N.; Hofer, R.; Ruiz-Taylor, L.; Textor, M.; Hubbell, J. A.; Spencer, N. D. *J. Phys. Chem. B* **2000**, *104*, 3298.
(12) Naderi, A.; Pettersson, T.; Makuska, R.; Claesson, P. M. *Langmuir* **2008**, *24*, 3336–3347.
(13) Lee, S.; Spence, N. D. *Langmuir* **2008**, *24*, 9479–9488.
(14) Lee, S.; Zürcher, S.; Dorcier, A.; Luengo, G. S.; Spence, N. D. *ACS Appl. Mater. Interfaces* **2009**, *1*, 1938–1945.
(15) Pettersson, T.; Dedinaite, A. *J. Colloid Interface Sci.* **2008**, *324*, 246–256.
(16) Naderi, A.; Makuska, R.; Claesson, P. M. *J. Colloid Interface Sci.* **2008**, *323*, 191–202.
(17) Naderi, A.; Iruthayaraj, J.; Pettersson, T.; Makuska, R.; Claesson, P. M. *Langmuir* **2008**, *24*, 6676–6682.
(18) Naderi, A.; Olanya, G.; Makuska, R.; Claesson, P. M. *J. Colloid Interface Sci.* **2008**, *323*, 223–228.
(19) Olanya, G.; Iruthayaraj, J.; Poptoshev, E.; Makuska, R.; Vareikis, A.; Claesson, P. M. *Langmuir* **2008**, *24*, 5341–5349.
(20) Iruthayaraj, J.; Poptoshev, E.; Vareikis, A.; Makuska, R.; van der Wal, A.; Claesson, P. M. *Macromolecules* **2005**, *38*, 6152–6160.
(21) Iruthayaraj, J.; Olanya, G.; Claesson, P. M. *J. Phys Chem. C* **2008**, *112*, 15028–15036.
(22) Linse, P.; Claesson, P. M. *Macromolecules* **2009**, *42*, 6310–6318.
(23) Postmus, B. R.; Leermakers, F. A. M.; Cohen Stuart, M. A. *Langmuir* **2008**, *24*, 1930–1942.
(24) Scheutjens, J. M. H. M.; Fleer, G. J. *J. Phys. Chem.* **1979**, *83*, 1619.
(25) Fleer, G. J.; Cohen Stuart, M. A.; Scheutjens, J. M. H. M.; Cosgrove, T.; Vincent, B. *Polymers at Interfaces*; Chapman & Hall: London, 1993.
(26) Linse, P. *Macromolecules* **1996**, *29*, 326–336.
(27) Leermakers, F. A. M.; Scheutjens, J. M. H. M. *J. Phys. Chem.* **1988**, *89*, 3264.
(28) Flory, P. J. *Principles of Polymer Chemistry*; Cornell University Press: Ithaca, NY, 1953.
(29) Karlström, G. *J. Phys. Chem.* **1985**, *89*, 4962–4964.